

Structural, Optical and Antimicrobial Activity of Cu Doped HAp: Synthesized by Solgel Method for Biomedical Applications

Saranya S*, Abinaya R, Padma R and Prema Rani M

Research Centre PG Department of Physics, The Madura College, Madurai-11, Tamilnadu, India

Research Article

Received: 12/07/2017

Accepted: 31/07/2017

Published: 12/08/2017

*For Correspondence

Saranya S, Research Centre PG
Department of Physics, The Madura
College, Madurai-11, Tamilnadu, India,
Tel: + 91 9444179205.

Email: saranyaashok122012@gmail.com

Keywords: Hydroxyapatite, FTIR, Copper,
Sol gel, XRD

ABSTRACT

Hydroxyapatite is the thermodynamically most stable crystalline phase of calcium phosphate in body fluid. Undoped hydroxyapatite (HAp) and two Cu substituted HAp samples with variable amounts (0.04 and 0.06)% of Cu were synthesized by sol-gel method. The samples were studied by X-ray diffraction (XRD), Fourier transform infrared (FTIR) spectroscopy and energy dispersive X-ray (EDX) spectroscopy to determine the crystallite size, functional groups and elemental composition respectively. The calculated dimensions of crystallites appeared to be within 25-59 nm. The average crystallite size derived from XRD data was observed to be reduced from undoped HAp to substituted HAp samples. The intensity of XRD peaks decrease from undoped HAp to Cu doped HAp. The bands at different modes are observed by FTIR spectrum. The band at 3641 cm^{-1} was also associated with the O-H stretching mode of the surface P-OH groups. The EDX results confirmed the composition of the doped and undoped HAp. The antimicrobial effects of doped hydroxyapatite powders against clinical pathogen *Shigella flexneri*.

INTRODUCTION

Hydroxyapatite (HAP), with the chemical formula of $\text{Ca}_{10}(\text{PO}_4)_6(\text{OH})_2$ and Ca/P ratio 1.67, is one of the most popular bioceramic materials. HAp bio ceramics have been widely used in medicine including dentistry and orthopedic applications. Various techniques such as sol-gel synthesis, solid-state reactions, chemical precipitation, have been developed to synthesize hydroxyapatite. Among the available methods, the sol-gel technique is a simple technique used to prepare nano structured HAp of high purity and crystallinity. Copper is essential to all living organisms as a trace dietary mineral. In humans copper is found mainly in the liver, muscle and bone. Copper containing enzyme called lysyl oxidase, copper aids in the formation of collagen for bone and connective tissue and contributes to the mechanical strength of bone collagen. In the present work, sol-gel method is used to synthesize both undoped HAP and Cu-doped HAP samples with variable amounts of Cu. The effect of Cu on the crystal structure, morphology and elemental composition of the HAP samples were investigated by X-ray diffraction (XRD), Fourier transform infrared (FTIR) spectroscopy, and energy dispersive X-ray (EDX) spectroscopy techniques [1,2].

EXPERIMENTAL PROCEDURES

Synthesis of Cu-doped Hydroxyapatite Nanoparticle

Cu-doped hydroxyapatite (Cu-HA) with different concentration (0, 4%, and 6%) of 0.1 M was synthesized by sol-gel method. The preparation of pure HAp was done by dissolving stoichiometric amount of Calcium nitrate tetrahydrate and Phosphorus pentoxide in 50 ml of ethanol in a separate beaker. Both the mixture were stirred for 40 minutes. Copper hydroxyapatite (Cu-HAp) was prepared by dissolving stoichiometric amount of Calcium nitrate tetrahydrate, Copper (II) nitrate pentahydrate and Phosphorus pentoxide in 150 ml of ethanol in a 200 ml beaker [3,4]. The mixture of sol was stirred vigorously on a magnetic stirrer for 40 minutes for uniform mixing. The resultant gel of both doped and undoped HAp was kept in water bath for 2 h to obtain precipitate. The precipitate was heated at 200°C to obtain powder. The obtained powder of Cu-HAp was then annealed at 650°C for 4 h. Finally the white powder was obtained.

RESULTS AND DISCUSSION

X-ray Diffraction (XRD)

The structural characterization has been done by XRD. X-ray powder diffraction measurements were performed using X-PERT PRO (Philips, Netherlands) at “The Sophisticated Analytical Instruments Facility (SAIF)”, IIT, Cochin using $\text{CuK}\alpha_1$ radiation with 2θ range from 20° to 120° and 0.02° step size. XRD profiles of the samples are given in **Figure 1**. The profiles were compared by the Joint Committee on Powder Diffraction Standards (JCPDS card no 030747). The pure HAp was with triclinic structure with lattice constants $a=6.906 \text{ \AA}$, $b=8.577 \text{ \AA}$, $c=6.634 \text{ \AA}$ and $\alpha=93.99^\circ$, $\beta=91.50^\circ$, $\gamma=127.6^\circ$. The average crystallite size (D) for the samples was estimated by the Scherrer equation, $D=k \lambda/\beta \cos\theta$, where k is the shape factor equal to 0.9, λ is the wavelength of X-rays ($\lambda=0.15406 \text{ nm}$ for Cu K α radiation), β is the full width at half maximum (FWHM) of X-ray reflection in the radians, and also θ is the Bragg’s diffraction angle in degrees. The results reported in **Table 1** show that the average crystallite size of Cu-doped samples is smaller than the value of undoped HAp. From the XRD peaks the intensity of the peaks decrease with increase in concentration of copper. The decrease in the intensity may be due to the valency of Cu which is one compared to that of phosphorus which is three. The decrease in intensity proceeds that the copper with lower ionic radius is doped with element with higher ionic radius (Ca) the volume density has been decreased correspondingly intensity also decreases. Furthermore crystallite size also decreases [5-7].

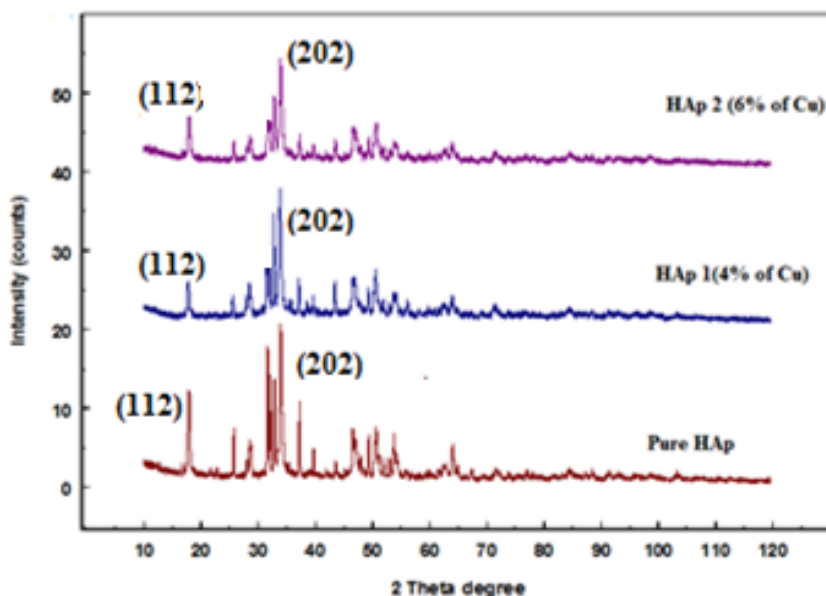


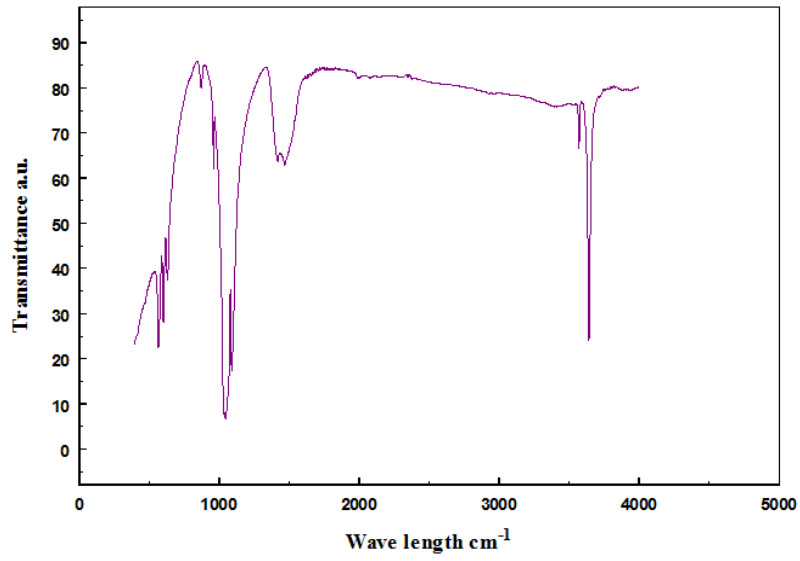
Figure 1. XRD Patterns of Pure HAp and Cu-HAp Nanoparticles and intensity variation in hkl plane.

Table 1. The average crystallite size of all the samples.

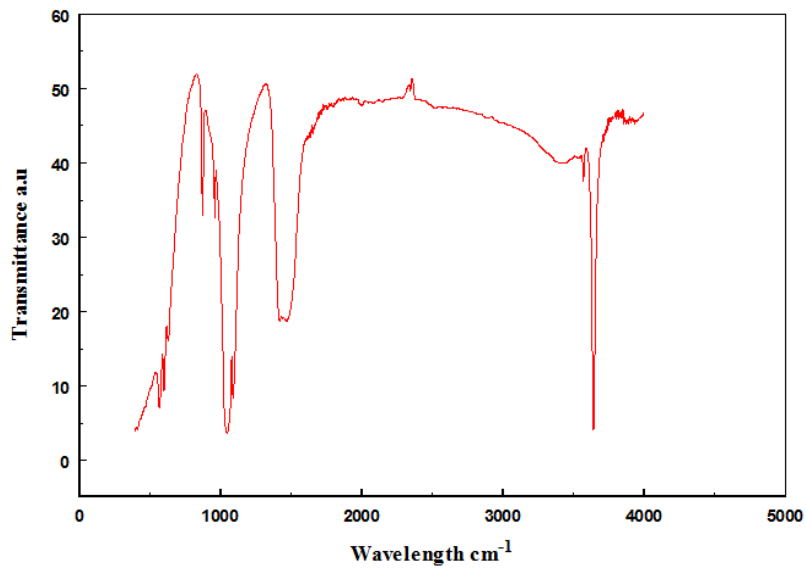
Sample	Grain Size (nm)
Pure HAp	59.41
Sample	Grain Size(nm)
Pure HAp	59.41

FTIR

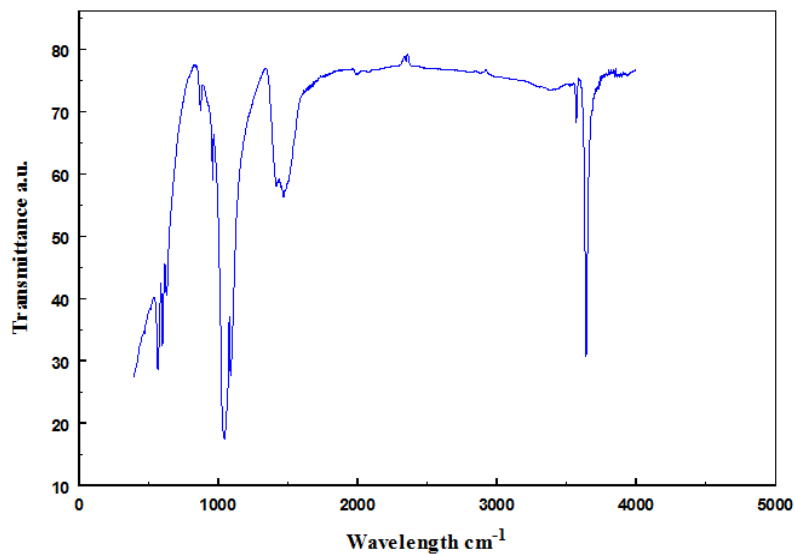
FTIR data collected from International Research centre (IRC) of Kalasalingam University with transmittance wavelength range 400 cm^{-1} to 5000 cm^{-1} . The obtained FTIR data are shown in **Figure 2.1** and a comparison of the data in **Figure 2.2**. The characteristic bands of phosphate and hydroxyl groups, as well as carbonate groups, were detected from the FTIR spectra of the samples. **Table 2** shows the Transmittance data from FTIR studies. The bands 3572 cm^{-1} , 3905 cm^{-1} and 3830 cm^{-1} confirms the presence of hydroxyl group of pure HAp, Hap 1 and HAp 2. The absorption band around 1421 cm^{-1} , 1469 cm^{-1} is attributed to the presence of CO_3^{2-} in all the samples. The intense broad peak between 962 cm^{-1} and 1047 cm^{-1} is assigned to PO_4^{3-} in samples Pure HAp, HAp1 and HAp2. The peak observed around 3572 cm^{-1} is the characteristic peak corresponding to stoichiometric Hap [7,8]. The extra peaks 3905 cm^{-1} , 3842 cm^{-1} were detected in HAp 2 (4% of Cu) and correspondingly 3830 cm^{-1} band was observed in HAp 3 (6% of Cu). Cu-HAP shows decreased intensity of OH vibration modes at those bands with respect to HAP samples. It can be explained by the increased lattice due to HPO_4^{2-} substitution. As seen in **Figure 2**, it is evident that the intensity of those peak decreases with increasing Cu content.



(i)



(ii)



(iii)

Figure 2. FTIR Transmittance spectrum of (i) Pure HAp (ii) HAp 1 (iii) HAp 2.

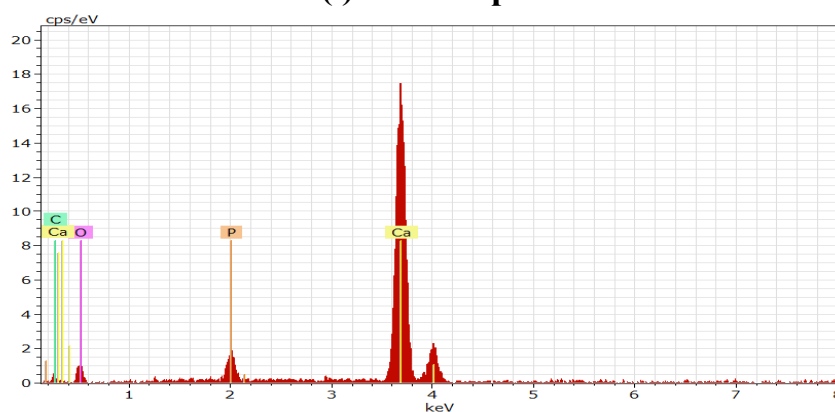
Table 2. Transmittance data of synthesized HAp Samples.

Samples	Bands (cm ⁻¹)	Groups	Modes
Pure HAp	3572,632	Hydroxyl (OH) ⁻	Vibrational
HAp 1(4%Cu)	3,90,53,842	Hydroxyl (OH) ⁻	Vibrational
HAp 2(6%Cu)	1,46,91,421	Carbonate (CO ₃) ²⁻	Asymmetric Stretching
HAp 2(6% Cu)	569	Phosphate (PO ₄) ³⁻	Asymmetric bending

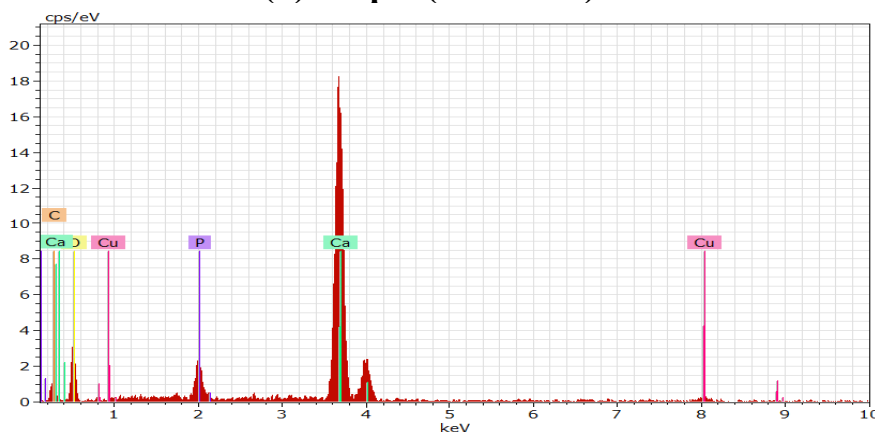
EDAX

The EDX spectra verify the elemental compositions and (Ca+Cu)/P molar ratios, and no impurity is observed for all the samples. Most importantly, the cu doping process causes the Ca-deficiency [9]. At higher amounts of the cu-dopants, the Ca-deficiency increases significantly. In other words, it may be due to the ionic substitution, which can be occurred due to crystal defect, between Cu and Ca. **Figure 3** shows the details about elemental composition of doped and undoped samples (**Table 3**).

(i) Pure HAp



(ii) HAp 1 (4% of Cu)



(iii) HAp 2 (6% of Cu)

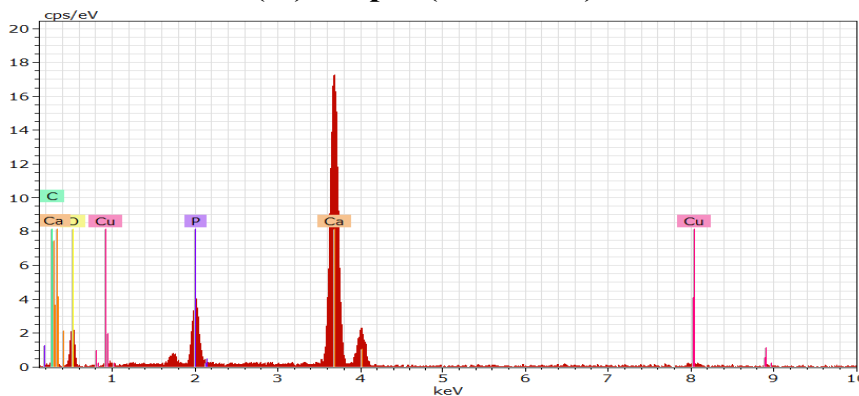


Figure 3. Elemental Composition of EDS Spectrum of Pure HAp, HAp1 and HAp2.

Table 3. Elemental composition of HAp and Cu-HAp nanoparticles.

Sample	Ca	P	C	O	Cu
Pure HAp	29.99	2.62	7.82	59.57	-
HAp 1(4% of Cu)	14.46	1.59	21.2	62.38	0.37
HAp 2 (6% of Cu)	19.74	3.96	7.43	68.36	0.52

Antibacterial Activity of the Extract of Compounds was Determined using Well Diffusion Method

It was performed by sterilizing Mueller Hinton agar media. After solidification, wells were cut on the Mueller Hinton agar using cork borer. The test bacterial pathogens were swabbed onto the surface of Mueller Hinton agar plates. Wells were impregnated with 25 µl of the test samples. The plates were incubated for 30 min to allow the extract to diffuse into the medium. The plates were incubated at 30 °C for 24 hours, and then the diameters of the zone of inhibition were measured in millimeters. Each antibacterial assay was performed in triplicate and mean values were reported (**Table 4**)^[10,11].

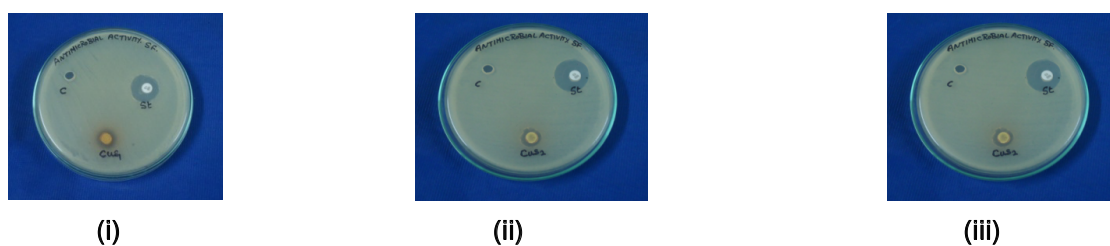


Figure 4. Antimicrobial activity of the compounds treated against *Shigella flexneri* with (i) pure HAp (ii) HAp1 (4% wt of Cu) (iii) HAp2 (6% wt of Cu).

Table 4. Antimicrobial activity of the Copper compounds treated against bacterial pathogens.

Test organism	Zone of inhibition in millimeter (in diameter)				
	Pure HAp	HAp 1 (4% of Cu)	HAp2 (6% of Cu)	Solvent control	Standard Nalidixic acid 30 µg
<i>Shigella flexneri</i>	17	14	19	NZ	25

The results of antibacterial activity of shigella flexneri- loaded hydroxyapatite. The zone of inhibition around Pure HAp against *Shigella flexneri* is given in **Figure 4i** and clear inhibition is found around HAp1 and HAp2 of 4%, 6% of Cu doped HAp against *Shigella flexneri* is given in **Figure 4**. The zone of inhibition increases with increase in Cu doped HAp with loaded test organism^[12-14]. The 6% Cu doped HAp nanoparticles have the greater antibacterial activity than pure HAp. Reading of results was carried by measuring width of the Zone of inhibition.

TEM analysis

Figure 5 shows the TEM Photographs of all synthesized samples annealed at 650 °C for 4 hours. It can be seen that the particles are more or less uniform in size and of spherical shape. The average crystallite size were calculated as 59-123 nm from TEM photographs^[15]. Based on the micrographs it can be concluded that the increase of the doping significantly affect the size and morphology of particles (**Table 5**).

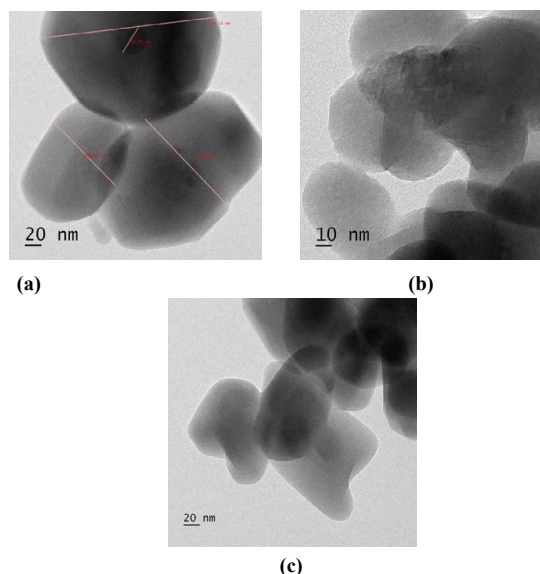


Figure 5. shows the TEM Photographs of (a) Pure HAp (b) HAp1 (0.04% Cu) (c) HAp2 (0.06% Cu) annealed for 650 °C for 4 hrs.

Table 5. The average crystallite size of all the samples.

Sample	Crystallite Size (nm)
Pure HAp	123
HAp 1 (4% of Cu)	63
HAp 2 (6% of Cu)	59

CONCLUSION

Sol-gel method is very useful to synthesize the Cu-containing bioceramics derived from hydroxyapatite. The analysis of XRD, FTIR and TEM showed that particles of all samples are of nano size and homogenous in composition. From the XRD data the crystallite size is observed to decrease with the increase content of Cu. This is because of decrease in volume density of the atom. The FTIR spectra proved formation of HAp due to the presence of hydroxyl and phosphate functional groups and intensity of peaks decreases in all the samples. The intensity of the band decreases by the addition of Cu dopant to the HAp. The Ca-deficiency occurs because of the Cu-doping process, and increases with addition of the dopants. Thus, prepared metal-doped hydroxyapatite nano powders can be applied as antimicrobial materials of various purpose such as for bone defects and implants coating in orthopedic surgery and for the treatment of skin infection.

REFERENCES

1. Park J. Bioceramics: properties, characterizations, and applications. Springer New York 2008.
2. Carter CB and Norton MG. Ceramic materials: science and engineering. Springer, New York 2013.
3. Hench LL. Bioceramics: from concept to clinic. *J Am Ceram Soc* 1991;74:1487-1510.
4. Chevalier J and Gremillard L. Ceramics for medical applications: a picture for the next 20 years. *J Eur Ceram Soc* 2009;29:1245-1255.
5. Ren F, et al. Chromium-based ceramic colors. *American Ceramic Society Bulletin* 1992;71:759-764.
6. Marinova Y, et al. Study of solid solutions, with perovskite structure, for application in the field of the ceramic pigments. *J Eur Ceram Soc* 2003;23:213.
7. Biqin C, et al. Fabrication and mechanical properties of β -TCP pieces by gel-casting method. 2008;28:1052-1056.
8. Raynaud S, et al. Calcium phosphate apatites with variable Ca/P atomic ratio I. Synthesis, characterisation and thermal stability of powders. *Biomaterials* 2002;23:1065-1072.
9. Berzina-Cimdina L and Borodajenko N. Research of Calcium Phosphates Using Fourier Transform Infrared Spectroscopy Riga Technical University, Institute of General Chemical Engineering, Latvia.
10. Chandrasekar A, et al. Synthesis and characterization of nano-hydroxyapatite (n-HAP) using the wet chemical technique. *Int J Phys Sci* 2013;8:1639-1645.
11. Osman Z and Arof AK. FTIR studies of chitosan acetate based polymer electrolytes. *Electrochimica Acta* 2003;48:993-999.
12. Susmita Bose and Susanta Kumar Saha. Synthesis and Characterization of Hydroxyapatite Nanopowders by Emulsion Technique. *Chem Mater* 2003;15:4464-4469.
13. Bigi A, et al. Hydroxyapatite gels and nanocrystals prepared through a sol-gel process. *J Solid State Chem* 2004;177:3092-3098.
14. Green D, et al. The potential of biomimesis in bone tissue engineering: lessons from the design and synthesis of invertebrate skeletons. *Bone* 2002;30:810-815.
15. Lawson AC and Czernuszka JT. Collagen-calcium phosphate composites. *Proc Instr Mech Eng* 1998;212:413-425.